



HAL
open science

Polyhydroxyalkanoate (PHA) based microfiltration membranes Tailoring the structure by the non-solvent induced phase separation (NIPS) process

P. Tomietto, M. Carré, Patrick Loulergue, L. Paugam, J.-L. Audic

► To cite this version:

P. Tomietto, M. Carré, Patrick Loulergue, L. Paugam, J.-L. Audic. Polyhydroxyalkanoate (PHA) based microfiltration membranes Tailoring the structure by the non-solvent induced phase separation (NIPS) process. *Polymer*, 2020, 204, pp.122813. 10.1016/j.polymer.2020.122813 . hal-02931994

HAL Id: hal-02931994

<https://hal.science/hal-02931994>

Submitted on 23 Nov 2020

HAL is a multi-disciplinary open access archive for the deposit and dissemination of scientific research documents, whether they are published or not. The documents may come from teaching and research institutions in France or abroad, or from public or private research centers.

L'archive ouverte pluridisciplinaire **HAL**, est destinée au dépôt et à la diffusion de documents scientifiques de niveau recherche, publiés ou non, émanant des établissements d'enseignement et de recherche français ou étrangers, des laboratoires publics ou privés.

**Polyhydroxyalkanoate (PHA) microfiltration membranes
processed by phase inversion.**

Pacôme Tomietto¹, Maewenn Carré, Patrick Loulergue¹, Lydie Paugam¹, Jean-Luc Audic^{1}*

¹ *Univ Rennes, Ecole Nationale Supérieure de Chimie de Rennes, CNRS, ISCR - UMR 6226, F-35000 Rennes, France.*

* *jean-luc.audic@univ-rennes1.fr*

Accepted manuscript

Abstract

Within the purpose of developing more sustainable membrane systems, it is herein proposed to implement a biobased and biodegradable material, the poly(hydroxybutyrate-co-hydroxyvalerate) (PHBV), to replace conventional polymers in a commonly used membrane fabrication process. The PHBV based membranes were made by non-solvent induced phase separation (NIPS) using N-methyl-2-pyrrolidone (NMP) as solvent. The process parameters and dope solution composition were developed in order to give structures suitable for performances characterization. In that sense, the microstructures were characterized in case of non-supported and supported membranes. The addition of hydrophilic additives, ethylene glycol (EG) and polyethylene glycol 300 g.mol⁻¹ (PEG300), was linked to the morphology changes. Porous asymmetric membranes were obtained in case of the non-supported membranes or supported membranes with a low amount of additive (1 wt%). Otherwise, symmetric porous membranes, made of interconnected crystal lamellas, were observed. The particularly high crystallinity of this biomaterial involved some different microstructures compared to classic polymers. Both types of structures demonstrated decent rejections of a clay dispersion. Due to the increased pore size, the permeabilities were greatly improved with the additives and values up to 480 L.m⁻².h⁻¹.bar⁻¹ were achieved.

Ταβλεοφ χοντεντο

1. Introduction	4
2. Materials and method	7
2.1. Chemicals	7
2.2. Hansen solubility parameters	7
2.3. Membrane preparation	8
2.4. Characterization	9
2.4.1. Scanning electron microscopy (SEM)	9
2.4.2. Porosity measurements	9
2.4.3. Membranes performances	9
2.4.3.1. Water permeability	10
2.4.3.2. Filtration of the kaolin dispersion	10
3. Results and discussion	11
3.1. Effect of the PHBHV concentration on the morphology and performances	11
3.1.1. Non-supported membranes	11
3.1.2. Supported membranes	14
3.2. Effect of additives on the morphology and performances	16
4. Conclusion	23
5. Conflicts of interest	24
6. Acknowledgements	24

1. Introduction

Nowadays, the membrane technologies are either replacing oldest purification systems thanks to their low energy requirement, or are bringing new separation solutions for novel applications. For instance, filtration membranes are playing a key role in facing the water scarcity while they are also involved in the development of new biomedical devices [1]. This has been possible thanks to the works of Loeb-Sourirajan who developed the non-solvent induced phase separation (NIPS) as a new technique to easily fabricate polymeric membranes with satisfactory performances [2]. Today, polymeric materials continue to be mainly used for membrane fabrication and account for 95% of the total membrane industrial market [3] and the NIPS fabrication technique is still the major processing method.

New membrane materials are constantly investigated within the purpose to bring better performances or to open up a wider scope of opportunities in terms of applications. However, most of the conventional polymeric materials intended for membrane fabrication are non-biobased and non-biodegradable. There are serious environmental concerns around the use of conventional polymers, such as consumption of the limited fossil resources, overgrowth of untreated wastes and environmental pollutions [4,5]. As a consequence, there is a rise of new legislations aiming to reduce their usage and/or to replace them by more sustainable alternatives. One of the best alternatives to these materials is the use of biopolymers, being either biobased, biodegradable or both [6]. In that sense, some literature studies pointed out the need to implement biopolymers as new materials to make more sustainable membranes [7-9].

Hence, some biopolymers such as polylactic acid [10-13], polybutylene succinate [14], alginate [15], starch [16], collagen [17], k-carrageenan [18], agarose [19] and gelatin [19] have been investigated to replace the current polymeric membrane materials within the existing applications. In addition, biopolymers can also bring new application opportunities thanks to their specific properties. It is, for example, the case of chitosan which demonstrated antibacterial properties [20-22].

In this study, a biopolymer belonging to the broad family of the polyhydroxyalkanoates (PHAs) was considered for membrane filtration applications. PHAs are linear homo- and co-polyesters produced from bacteria, they are biodegradable and have versatile properties. Their chemical structure depends on their production conditions and the resulting thermomechanical properties of the macromolecule is hence strongly influenced [23-25]. The homopolymer

polyhydroxybutyrate (PHB) and the copolymer poly(hydroxybutyrate-co-hydroxyvalerate) (PHBHV) (Figure 1) are the two most produced PHAs [26]. Both have a high degree of crystallinity [24]. Nevertheless, PHBHV is usually preferred to PHB due to its better flexibility.

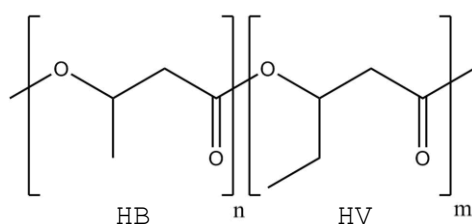


Figure 1: Chemical structure of PHBHV

PHAs have been considered for several different application fields, like the medical sector [27–29], cosmetics [30], packaging [23,31–34] or toys [35]. Depending on the targeted applications and the expected material structure, PHA was processed by different techniques, including by phase inversion (Table 1). This technique is based on the evolution of a thermodynamic equilibrium starting from a polymeric dope solution to form a solid structure. It can be achieved through different ways: solvent evaporation (evaporation induced phase separation, EIPS), temperature change (temperature induced phase separation, TIPS), liquid non-solvent addition (non-solvent induced phase separation, NIPS) or vaporized non-solvent addition (vapor-induced phase separation, VIPS). Thanks to the thermodynamic equilibriums and kinetic involved during the process, various structures, from dense to porous, and from symmetric to asymmetric can be obtained. Hence, it is possible to tailor the material microstructure by playing with the dope solution composition and the process parameters. However, if this technique has been well developed for classic polymers, when new materials with different properties are involved, the phase inversion process has to be re-investigated. Indeed, in this case, PHAs are known for their high crystallinity degree, what may significantly impact the phase separation behavior and hence the final microstructure.

Table 1: Solvents used in the literature to process PHAs via phase inversion.

Solvent	Phase inversion technique	Application	Reference
Also used for membrane fabrication	N-Methyl-2-pyrrolidone (NMP)	NIPS, VIPS	Antibiofilm material [36,37]
	1,4-Dioxane	TIPS	Biomedical [38,39]
	Chloroform	EIPS, NIPS	Biomedical, Membranes [40,41,50–53,42–49]
Others	Methyl isobutyl ketone (MIBK)	EIPS	Antibiofilm material [54]
	Methylene	EIPS	Biomedical [55]

Chloroform has been mainly used for the phase inversion of PHAs since it is the best solvent for their solubilization [56]. This is due to a polar interaction between the chlorine and the carbonyl carbon, associated with a hydrogen bonding between the hydrogen on chloroform and the carbonyl oxygen. By using this solvent, PHA films with porous to dense structures could be obtained [40,41,50-53,42-49]. PHA based membranes intended either for pervaporation or water filtration, have also been reported. In case of pervaporation applications, the membranes were made by a simple EIPS to achieve dense structures [41]. In case of water filtration applications, porous structures were obtained by combining EIPS with NIPS [40]. Since chloroform is not soluble in water, the coagulation baths were mainly made of ethanol. If NIPS is a suitable method for high scale membrane fabrication, this fabrication technique would not be relevant for a scale up as chloroform is a highly hazardous chemical and ethanol has also health hazards.

The EIPS technique was also performed with methyl isobutyl ketone (MIBK) and methylene chloride to make films with an antibiofilm activity or for biomedical applications [54,55]. Porous structures could be obtained by changing the dope solution composition and the nature of the polymer. However, EIPS is not the best technique to recover and recycle the solvent. In addition, because MIBK and methylene chloride are only slightly soluble in water, it is not possible to use them for the NIPS method with water as coagulation bath.

The TIPS method was performed with 1,4-dioxane [38,39]. Porous structures intended for biomedical applications were made. Different microstructures were obtained depending on the cooling temperature and polymer concentration. However, additionally to its health hazards, 1,4-dioxane suffers from being highly flammable.

Finally, non-solvent induced phase separation via NIPS or VIPS were performed with N-methyl-2-pyrrolidone (NMP) [36,37]. A few phase inversion parameters were studied in case of the NIPS process. The structures were intended as support for additional anti-biofilm materials [36]. Then, the same authors studied the VIPS technique by changing various phase inversion parameters [37]. The VIPS technique is actually very similar to NIPS since it also requires the use of water as a non-solvent.

If PHAs have often been processed by phase inversion to tailor the material microstructure, it has never really been investigated for membrane filtration applications. As described, porous microstructures have been previously obtained with NMP as solvent using NIPS or VIPS. The NMP and NIPS are one of the most frequently

used solvent [57] and technique for membrane fabrication so that the fabrication scales up could be easily considered. Thus, NMP is prone to be investigated as a NIPS solvent for the fabrication of PHA based membranes intended for filtration applications.

Herein and for the first time, PHBHV based membranes intended for water filtration were made by NIPS using NMP as solvent. Both supported and non-supported membranes were made. The influence of the polymer concentration and different additives on the microstructure was investigated. Polyethylene glycol (PEG) and ethylene glycol (EG) were added at different concentrations playing the role of pore former. The membranes microstructures were characterized by scanning electron microscopy (SEM) images, pore size distribution and porosity. In order to demonstrate their potential as filtration membranes, the performances were evaluated in terms of pure water permeability and filtration of a kaolin dispersion. Finally, the filtration performances were correlated to the membranes microstructures.

2. Materials and method

2.1. Chemicals

The PHBHV pellets, sold under the trade name Enmat Y1000P, were purchased from Tianan Biologic Material. The pellets were purified by a first solubilization in chloroform followed by a precipitation in methanol. The obtained white purified PHBHV powder was characterized by gel permeation chromatography made of three successive columns, 2 × ResiPore and 1 × PL gel Mixed C (Agilent), ended with a Waters UV detector working at 241nm. The weight average molecular weight (M_w) was determined using a calibration curve of polystyrene standards. $M_w = 116\ 000\ \text{g}\cdot\text{mol}^{-1}$. The crystallinity degree (χ_c) was determined by differential scanning calorimetry with the apparatus Q10 DSC from TA Instruments. $\chi_c = 62\%$. The ratio of hydroxyvalerate (HV) was determined by ^1H NMR analysis with a Bruker 400 MHz apparatus. HV = 3 mol%.

Polyethyleneglycol 300 $\text{g}\cdot\text{mol}^{-1}$ (PEG300) and ethylene glycol (EG) were supplied by VWR (U.S.). N-methyl-2-pyrrolidone (NMP) was supplied by Prolabo (99% purity). These chemicals were used as received.

The non-woven membrane support is made of polypropylene/polyethylene fibers. It is commercially available under the trade name Novatexx 2471 and was kindly provided by the Freudenberg company.

The kaolin clay was supplied by Prolabo.

2.2. Hansen solubility parameters

Further in the discussion, the affinities between the different chemicals is described using the δ_v - δ_h diagram. This 2D-diagram has been reported as a relevant easy way to represent the molecular

interactions [58,59]. The δ_v and δ_h values are extracted from the Hansen solubility parameters (HSP). δ_h corresponds to the hydrogen bonding parameter and δ_v , introduced by Bagley *et al.* [59], is the association of both dispersion parameter (δ_d) and polarity parameter (δ_p). δ_v is calculated as follow:

$$\delta_v = \sqrt{(\delta_d^2 + \delta_p^2)}$$

The values of the considered chemicals are displayed in Table 2 with the HSP parameters extracted from the literature [59-61].

Table 2: Hansen's parameters of the involved chemicals during the membrane fabrication.

Chemical		δ_d (MPa ^{1/2})	δ_p (MPa ^{1/2})	δ_h (MPa ^{1/2})	δ_v (MPa ^{1/2})
Polymer	PHB	15.5	9.0	8.6	17.9
Additives	PEG300	16.6	4.4	14.5	17.2
	EG	17.2	12.7	26.8	21.4
Solvent	NMP	18.0	12.3	7.2	21.8
Non solvent	Water	15.6	16.0	42.3	22.3

Regarding the low HV ratio (3 mol%) within the PHBHV herein used, PHB is considered as an accurate representation of the PHBHV molecule. Hence, the HSP values of PHB, available in the literature, were used to represent the HSP values of this PHBHV [60].

2.3. Membrane preparation

The PHBHV based membranes were prepared by solution casting followed by NIPS. First, homogeneous dope solutions were prepared by dissolving the purified PHBHV powder and additives in NMP at 120°C for 4 hours. The different compositions of the herein studied membranes are noted in Table 3. The dope solutions were then cooled down to 100°C and casted with a thickness of 250 μ m. The solutions were casted either directly on a glass plate at 25°C (non-supported membranes) or on the non-woven support taped on the glass plate at 25°C (supported membranes). The glass plate is then directly placed in the non-solvent bath containing 2.5L of demineralized water at 20°C for 20min. Then, the obtained membranes are stored in demineralized water in a fridge regulated at 5°C.

Table 3: References of the various fabricated membranes. Concentrations are in weight percentage (wt%) in respect to the total dope solution.

Membrane reference	Supported	PHBV concentration (wt%)	Additives	
			Nature	Concentration (wt%)
NS PHBV15	No	15	None	
NS PHBV20		20		
NS PHBV25		25		
PHBV25	Yes	25	None	
PHBV30		30		
PHBV/1%PEG300	Yes	25	PEG 300	1
PHBV/2%PEG300				2
PHBV/5%PEG300				5
PHBV/1%EG			EG	1
PHBV/2%EG				2

2.4. Characterization

2.4.1. Scanning electron microscopy (SEM)

SEM images of the membranes surface and cross-section were performed with a JSM-7100F apparatus from JEOL. The acceleration voltage was 5.0 kV. In case of the cross section analyzes, the membranes were fractured after liquid nitrogen cooling. The samples were coated with a gold/palladium mixture.

2.4.2. Porosity measurements

For the non-supported membranes, because of their fragility, only the surface porosity could be analyzed. The surface porosity was measured by analysis of the SEM images having a magnification of 2500. With the ImageJ software, the brightness and contrast of each image were adjusted in order to define the pores as black pixels. Then, the surface porosity was determined using the analyze particles function. The mean of two measurements was performed.

The overall porosities of the supported membranes were analyzed using a mercury intrusion porosimeter. The AutoPore IV 9500 apparatus from Micrometrics was used. The entire membrane was introduced into the capillary. The influence of the support, having much bigger pores than the selective layer, was extracted from the porosity characterizations by selecting the proper intrusion pressure range. The intrusion pressure range was from 17 PSI (117.10^3 Pa) to 60.10^3 PSI (413.10^6 Pa).

2.4.3. Membranes performances

Membranes performances were characterized by first measuring the water permeability followed by the filtration of a kaolin dispersion (rejection test).

To fit the filtration cell, circular coupons were cut from the membranes using a cutting knife of 44mm diameter. The coupons were soaked into demineralized water 12 hours prior to the tests. The filtration set up is displayed on Figure 2. The filtration cell was a dead-end Amicon stirred cell of 50 mL (model 5122) with a filtration area of 12.6 cm². A 5L inox container, from Sartorius Stedim Biotech, was added upstream to the cell to ensure sufficient volumes of feed. The transmembrane pressure was ensured by pressurized air and managed with a pressure regulator.

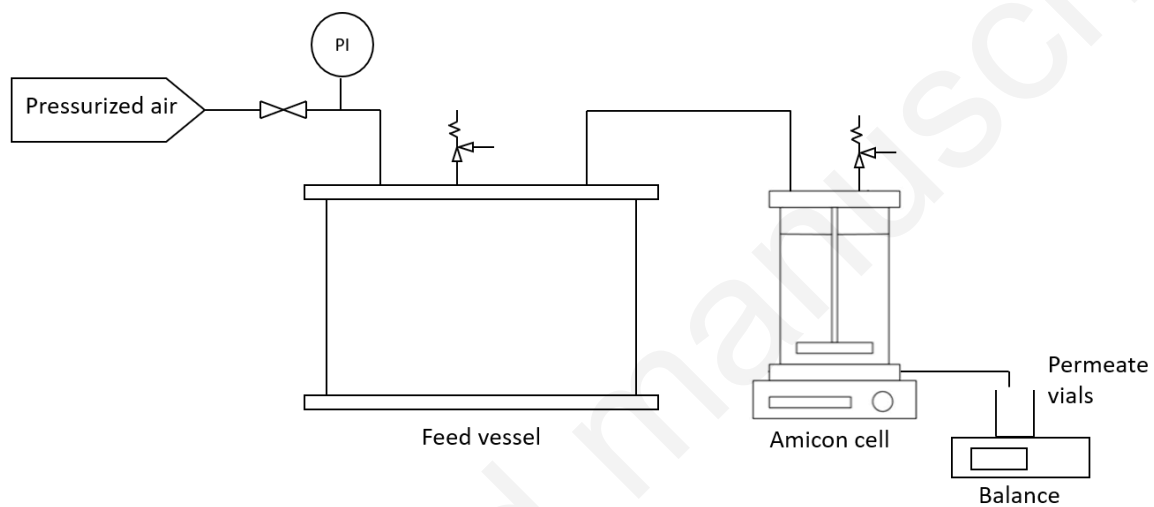


Figure 2: Schema of the filtration set up for the determination of the water permeability and kaolin rejection.

2.4.3.1. Water permeability

The permeability was measured with demineralized water at 22°C. The membranes were compacted with a transmembrane pressure of 2 bars until flux stabilization. The water permeability (L_p , L.m⁻².h⁻¹.bar⁻¹) was calculated by mean of three measurements and using the following formula:

$$L_p = \frac{Q}{S \times TMP}$$

Q being the water flux (L.h⁻¹), S the membrane surface (m²) and TMP the transmembrane pressure (bar).

2.4.3.2. Filtration of the kaolin dispersion

Kaolin dispersions were prepared by mixing 0.4 g of kaolin in 800 mL of demineralized water. The dispersion was then stirred for 15 min and place in a sonification bath for 10 min. Next, the dispersion was centrifugated for one hour to settle down the unstable

particles. Finally, the supernatant was kept as the feed for the rejection test. The feed concentration was always within the range of 110-150 g.L⁻¹. A diffracted light scattering analysis was performed over 1 hour in order to measure the particles size and their stability. The size of the particles was 0.65 ± 0.03 μm and no major change was observed along this period. About 200 mL of the dispersion was filtered through the investigated membrane. The concentration in the feed and permeate was measured by gravimetric analyzes.

Then, the rejection was calculated as:

$$R = \left(\frac{C_{\text{feed}} - C_{\text{permeate}}}{C_{\text{feed}}} \right) \times 100$$

Where C_{feed} and C_{permeate} are respectively the kaolin dispersion concentrations, in the feed and permeate.

3. Results and discussion

3.1. Effect of the PHBHV concentration on the morphology and performances

3.1.1. Non-supported membranes

The membranes were firstly prepared without any support. The influence of the PHBHV concentration into the dope solution was investigated. Figure 3 displays the SEM images of membranes prepared from PHBHV concentrations from 15 wt% to 25 wt%. These concentrations are within the range of what is commonly used for the membrane fabrication by NIPS [62].

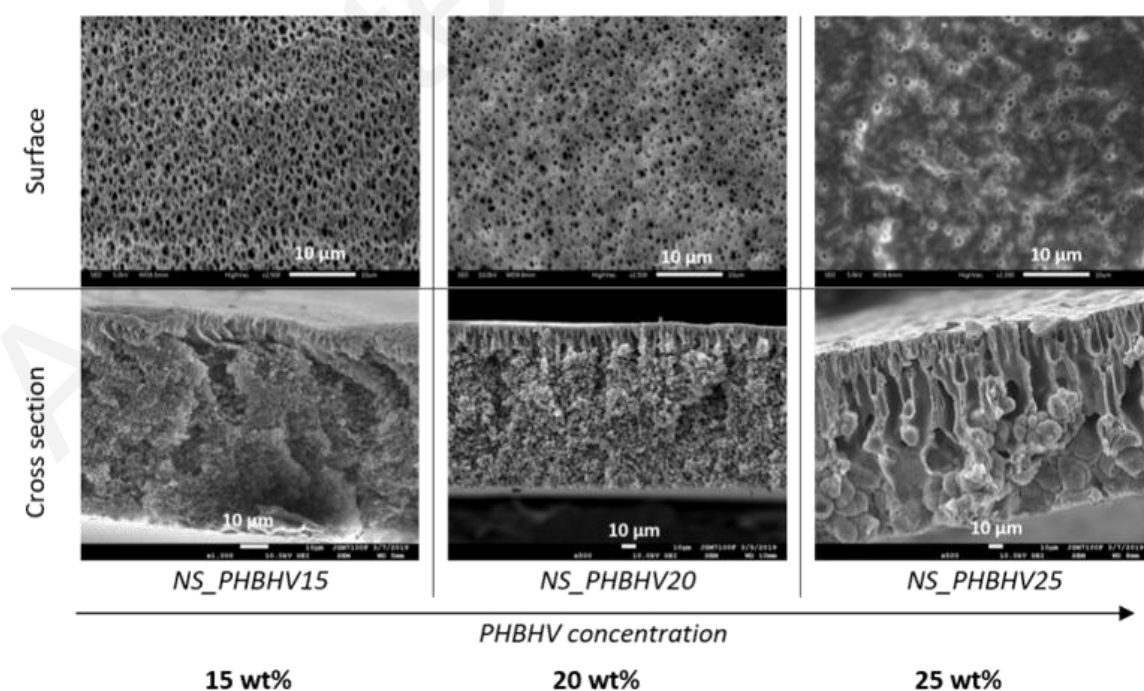


Figure 3: SEM images of the non-supported membranes prepared with different PHBV concentrations. Surface and cross-sectional images.

For all the compositions, asymmetric cross-section structures with a finger like upper layer and a sponge like sublayer can be observed. This is a commonly obtained microstructure for the membranes made from this NIPS process [62-66]. Due to the immersion into the coagulation bath, the exchange between the solvent and non-solvent creates a thermodynamically unstable solution leading then to the demixing process [65]. Additionally to the thermodynamic aspect, the kinetic aspect (mass transfer) also strongly influences the separation process. At the end, these asymmetric microstructures are the result of a complex competition between the different demixing mechanisms through the solution thickness.

The top surface first quickly precipitates due to the direct contact with the coagulation bath. Usually, it results in a dense skin layer. This dense skin layer is the consequence of a rapid spinodal demixing [64]. However, porous top layers are herein observed. Hence, it could be argued that despite the direct contact with the coagulation bath, the top surface undergoes a L-L demixing by nucleation and growth (NG) of the polymeric lean phase. In that case, the polymeric lean phase would form the final pores while the solidification of the polymeric rich phase makes the membrane matrix. Then, finger like macrovoids are formed beneath the top surface.

Different theories were formulated to describe the formation origin of the finger like macrovoids [64,66,67]. According to Strathmann *et al.*, the macrovoids result from the rapid penetration of non-solvent through weak spots in the top layer [67]. In the present case, the weak spots would be the surface pores. The finger continues to grow until the precipitated polymer at the bottom of the finger can no longer be easily moved. This theory mainly takes into consideration the solvent/non-solvent exchange rate. But according to the theory of Smolders *et al.*, macrovoids are due to the formation of freshly nuclei of the polymeric lean phase formed beneath a dense skin layer [64]. These nuclei have a high amount of solvent and can be considered as local coagulation bath with a lot of solvent [66]. Then, the solvent diffusion from the surrounding into the nuclei causes the growth and formation of the final macrovoids. Hence, additionally to the solvent/non-solvent exchange rate, this theory also takes into consideration the relative kinetic of the growth of polymer lean phase nuclei.

Independently of the theory explaining the macrovoids origin, it is sure from the experimental results that a fast solvent/non-solvent exchange rate is required for their formation [63]. For example, a good solvent/non-solvent miscibility, like here NMP/water, favors the formation of these finger like macrovoids [65,68].

Nevertheless, the surface porosity and the size of the finger like structures change as a function of the PHBHV concentration. To quantify these changes, more detailed structural analyzes are shown in Table 4.

Table 4: Structural properties of the non-supported PHBHV membranes. Influence of the PHBHV concentration.

Membrane	Thickness (μm)		Thickness ratio Finger like/Overall (%)	Surface porosity (%)
	Overall membrane	Finger like structure		
NS_PHBHV15	77 ± 2	8 ± 1	10 ± 1	16.9 ± 0.9
NS_PHBHV20	113 ± 1	19 ± 2	17 ± 2	7.7 ± 0.3
NS_PHBHV25	130 ± 3	72 ± 17	55 ± 13	2.9 ± 0.1

As observed on Figure 3 and correlated to the values in Table 4, the increase of PHBHV concentration tends to decrease the surface porosity, increases the membrane thickness and increases the fingers length. Considering the nucleation and growth mechanism for the top surface formation, a higher polymer concentration generates a higher polymeric rich phase volume and lower polymeric lean phase volume. Since the polymeric lean phase finally makes the pores, if its volume is lowered, the volume of pores is lowered too. That is why the surface porosity decreases when the polymer concentration increases.

Considering the cross section, a lower polymer concentration usually leads to bigger finger like macrovoids [63]. Indeed, a lower polymer concentration gives a lower solution viscosity inducing a faster solvent/non-solvent exchange rate. However, an opposite trend is observed in this case.

Considering the formation theory of Strathmann *et al.*, the macrovoids size is strongly dependent of the non-solvent income passing through the surface pores. Hence, a higher surface porosity would increase this phenomenon and promote the macrovoids formation. But this is not what is observed here. The membrane with the higher surface porosity has the smaller finger like macrovoids. Then, to explain this, the theory of Smolders *et al.* has to be considered. As mentioned above, this theory considers the growth of a nuclei made of a polymeric lean phase. A more delayed demixing gives more time to the nuclei to grow and to form bigger macrovoids. So, when the polymer concentration is increased, the decreased surface porosity reduces the non-solvent income into the membrane thickness and finally give a delayed demixing. Hence, bigger macrovoids are formed when the concentration is increased.

For filtration applications, such asymmetric finger like structures would favor high fluxes, owing to the draining effect of the macrovoids, while keeping the sieving rejection thanks to the top surface. Unfortunately, these membranes exhibited poor mechanical properties, hindering their use for further filtration tests. These mechanical weaknesses may be explained by the poor mechanical properties associated to the macrovoids [69] but the nature of the polymer can be involved too. In this case, a PHBV with a crystallinity of 62% was used. This high degree of crystallinity may be the reason of a brittleness and poor mechanical properties [33]. One solution to this problem would be the use of a PHA with a higher HV content or longer side chain length, offering a lower crystallinity degree. But such PHAs are, at that time, less available on a commercial scale. Hence, in order to overcome this mechanical issue and be able to investigate the filtration behavior of such PHA based membranes, the same investigations were applied to supported membranes.

3.1.2. Supported membranes

To make supported PHBV based membranes, dope solutions were casted on a non-woven support taped on a glass plate. Similarly to the previous part, the effect of the PHBV concentration was firstly investigated. For these supported membranes, a minimum concentration of 25 wt% was necessary. For the lower concentrations, due to lower viscosities, the dope solutions penetrated the support before the phase inversion occurs. Hence, two different concentrations, 25 wt% and 30 wt%, are herein studied. These membranes are named respectively PHBV25 and PHBV30. Figure 4 shows their SEM images.

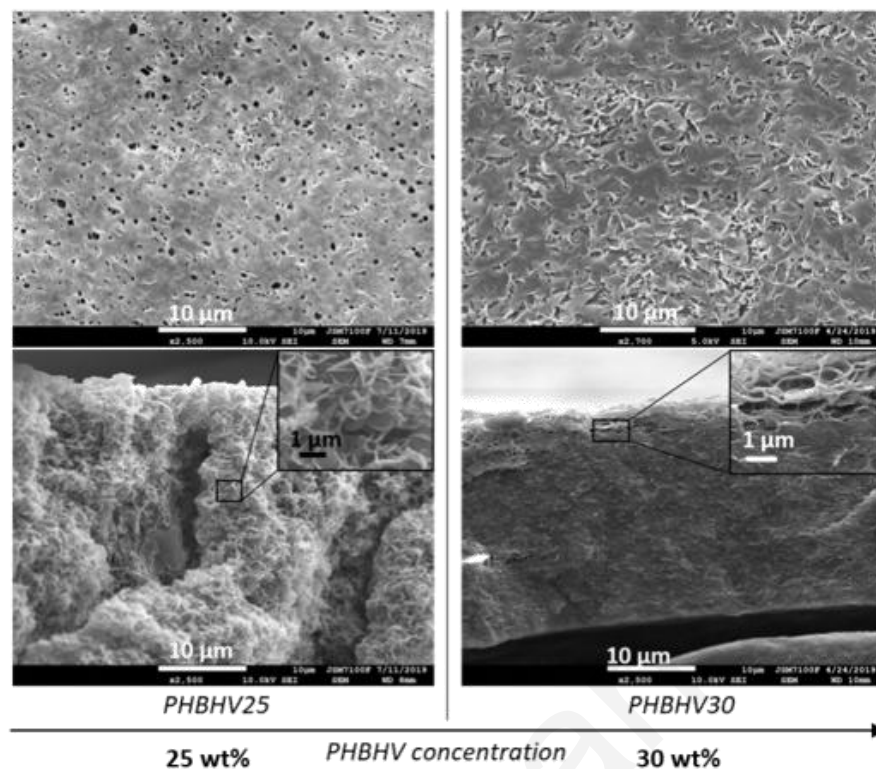


Figure 4: SEM images of the membranes selective layers prepared with different PHBV concentrations. Top and bottom images are respectively surface and cross-sectional images.

The PHBV25 membrane shows a porous top surface and a symmetric leafy bi-continuous cross section. This leafy structure is actually made of interconnected crystal lamellas resulting from a solid-liquid (S-L) demixing [70]. Indeed, in case of crystalline polymers, the solid-liquid demixing may precede the liquid-liquid (L-L) demixing when the latter is sufficiently delayed [71]. This late L-L demixing is usually promoted in case of high polymer concentration or low coagulation bath temperature [72]. That is why the S-L demixing usually happens for membranes made by TIPS [63,73]. Since the dope solution, initially at 100°C, is cooled down to 20°C when introduced into the coagulation bath, it could be expected that a TIPS occurred in parallel to the NIPS during the membrane fabrication process [63]. Plus, the insoluble crystalline parts present into the dope solution [74] may act as nucleating agent during the membrane crystallization, what favors the formation of small interconnected crystals, and hence leads to this leafy structure [70,75].

Nevertheless, by comparing the non-supported membrane (Figure 3) to the supported membrane (Figure 4) made with the same 25 wt% PHBV concentration, two different structures are observed. In case of the non-supported membrane, a finger like structure resulting from a L-L demixing is observed. While a leafy structure resulting from a S-L

demixing is observed for the supported membrane. Hence, it seems that the support impact the final structure by potentially reducing the L-L demixing rate during the phase inversion.

When the polymer concentration is increased to 30 wt% the resulted membrane displays a denser surface structure and a dense cross section. But still, some crystals lamellas are visible, what also confirms the S-L demixing. Indeed, the S-L demixing is even more predominant at higher polymer concentration [72]. Here, the concentration is so important that there are much more connections between crystals, leading to this much denser structure. Hence the porosity is reduced by increasing the concentration (Table 5). The membrane thickness is also reduced when the concentration is increased, what could be explained by the reduced porosity (Table 5).

Table 5: Structural properties of the supported PHBHV membranes. Influence of the PHBHV concentration.

Membrane	Membrane thickness (μm)	Overall porosity (%)	L_p ($\text{L.m}^{-2}.\text{h}^{-1}.\text{bar}^{-1}$)	Rejection (%)
PHBHV25	79 ± 9	41 ± 2	29.2 ± 4.9	83.8 ± 1.7
PHBHV30	25 ± 1	25 ± 1	2.5 ± 0.4	-

Compared to the non-supported membranes, here the mechanical backing brought by the non-woven support make the overall structure suitable for the membranes performances tests. PHBHV25 membrane displays a water permeability of $29.2 \text{ L.m}^{-2}.\text{h}^{-1}.\text{bar}^{-1}$ and a rejection of kaolin particles ($0.65 \mu\text{m}$) of 83.8%. Due to its lower porosity, the PHBHV30 membrane has a lower permeability. The rejection behavior of PHBHV30 membrane was not evaluated because of its poor permeability.

These firsts performance results highlight the ability of these PHBHV based membranes to be used for filtration application. However, these values are very low. In order to improve the permeability, the effect of hydrophilic additives potentially acting as pore former agents was studied.

3.2. Effect of additives on the morphology and performances

In order to improve the membrane performances, additives were added into the dope solution. The PHBHV25 membrane was used as reference since it displayed a higher permeability value compared to PHBHV30. Hence, the PHBHV concentration was set at 25 wt%. PEG300 and EG were chosen as additives. These additives are both soluble in NMP and water. PEGs have been widely used for membrane fabrication [76-80] and act as pore former agents and hydrophilic additives [76], thus promoting the membrane permeability. Nonetheless, PEGs from 200 to 4000 g.mol^{-1} have already been intensively used as plasticizers for PHA based materials [81,82], so the pore former effect of PEG300

could be counter balanced by its plasticizing effect. That is why EG was also studied as additive. Figure 5 displays the δ_v - δ_h diagram for the involved chemicals in the studied membranes. The closer are the points, the greater is the affinity between the chemicals.

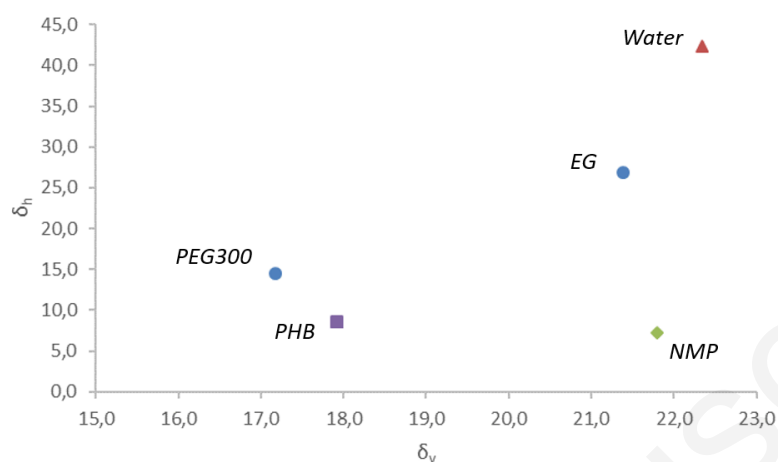


Figure 5: δ_v - δ_h diagram for the involved chemicals in the studied membranes.

As seen on Figure 5, compared to PEG300, EG has a smaller molecular size but also a higher affinity with water. It should promote a better leaching out during the phase inversion. If the chemical structures between the additives are similar, the molecular weight changes so the OH end groups contribution will be smaller for PEG300 than for EG. Hence, their hydrogen bonding parameters (δ_h) are different [61] and the EG presents a higher affinity with water.

PEG300 and EG were added at different concentrations ranging from 1 wt% to 5 wt% into the dope solution. Figure 6 shows the SEM images of membranes made with 1 wt% of additive.

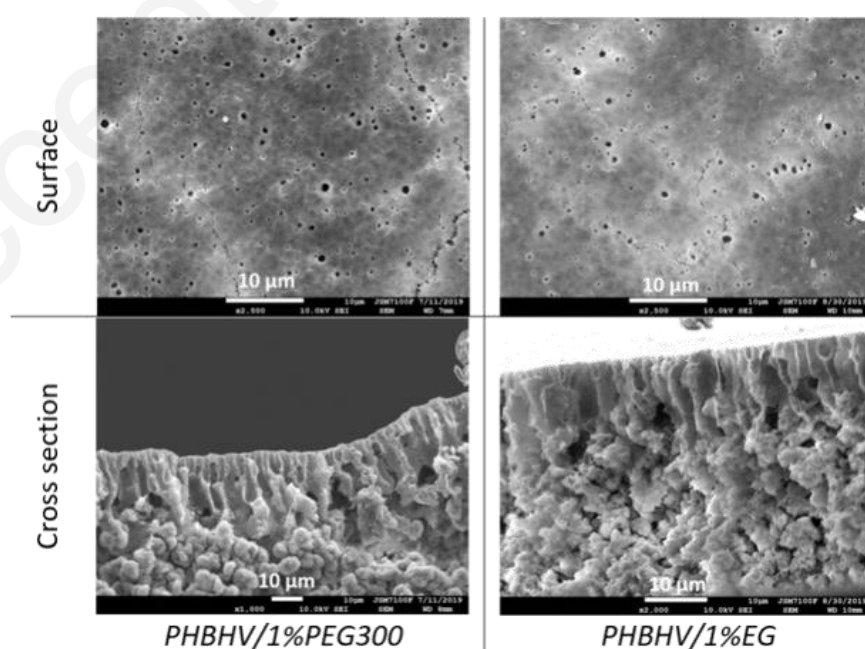


Figure 6: SEM images of the membranes prepared with 1 wt% of PEG300 and EG. Surface and cross-sectional images.

The membranes have a porous surface, what was also the case for the PHBHV25 membrane without additive. However, these membranes have major changes regarding the cross-section microstructure. The membranes with 1 wt% of additive exhibit a finger like upper structure and a spherulitic sublayer. This combination of structures was described as a competition between a NIPS and TIPS process [63]. As described previously, the NIPS process and L-L demixing is responsible of the finger like macrovoids formation and is favored in case of fast exchange rate between the solvent and non-solvent. Because the macrovoids were not observed for the membrane without additive (Figure 4), it seems that adding 1 wt% of PEG300 or EG tends to favor the formation of macrovoids. This phenomenon has been reported in the literature as a consequence of two phenomena. First, because of the shift of the dope solution composition closer to the binodal curve, thus inducing a faster demixing [63]. And secondly because of the additive hydrophilicity favoring the non-solvent (water) influx [79,83].

The spherulitic sublayer is a consequence of a S-L demixing induced by the polymer crystallization [63,73]. As explained above in paragraph 3.1.2, due to the polymer crystallinity and the cooling down from 100°C to 20°C during the coagulation bath step, the TIPS process may occur hence giving this spherulitic structure.

But the association of finger like macrovoids with a spherulitic structure may impact the mechanical property of the membrane. Indeed, macrovoids are known to weaken the structure [69] and such big spherulites too. In fact, a lack of connections between spherulites can reduce the substructure cohesion and consequently decrease the mechanical strength [63]. Thus, the recent investigations on the TIPS process were focused on producing a bicontinuous structure [72,75]. That is why bicontinuous structures similar to the one observed for PHBHV25 membrane are more suitable. And this type of microstructure was actually obtained for additive concentrations above 1 wt%.

Figure 7 shows the SEM images of membranes made with 2 wt% and 5 wt% of additives. The case of the membrane made with 5 wt% of EG is not displayed here. Indeed, after the fabrication process the membrane presented to many visual defects. Since EG has a lower affinity with NMP and PHB, compared to PEG300, at this 5 wt% concentration a phase segregation may take place during phase inversion thus leading to the formation of defects.

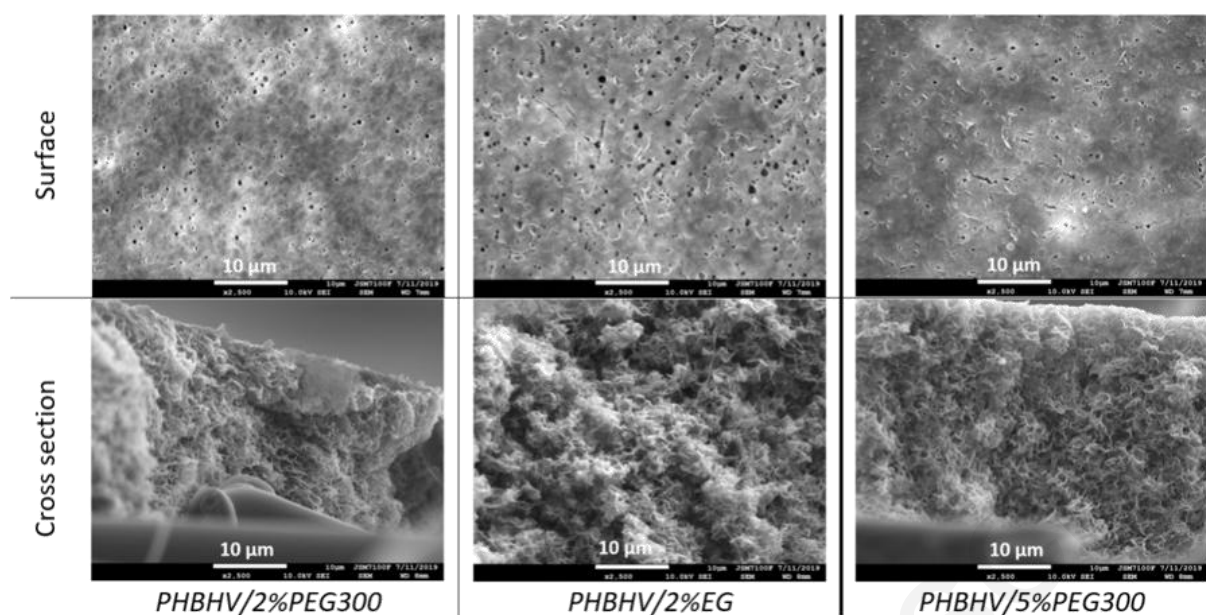


Figure 7: SEM images of the membranes prepared with 2 wt% or 5 wt% of PEG300 or EG. Surface and cross-sectional images.

By increasing the additive concentration to 2 wt% and 5 wt%, the morphology changes again to a leafy structure made of interconnected crystal lamellas, like the one obtained for PHBHV25 membrane. By adding more additive, a higher finger like structure could have been expected, since more hydrophilic additive was added [79]. However, it is not the case here and this leafy structure suggests a dominating S-L demixing due to a non-instantaneous L-L demixing. It was previously reported that macrovoids are hindered when the concentration of additive exceed a certain minimum value [36,79,84]. Indeed, further addition of additive can increase the solution viscosity and hence reduces the solvent/non-solvent exchange rate [36,79]. Then, thanks to the delayed exchange rate, S-L demixing by crystallization may overcome the L-L demixing and finally leads to these leafy structures. Between 2 wt% and 5 wt% of PEG300, no major difference is noticed from the SEM analyzes.

More detailed microstructure analyzes are mentioned in Table 6.

Table 6: Thickness and porosity of PHBHV based membranes with PEG300 or EG as additives.

Membrane	Thickness (μm)		Thickness ratio Finger like/Overall	Overall porosity (%)
	Overall membrane	Finger like structure		
PHBHV25	79 ± 9	No finger like structure		41 ± 2
PHBHV/1%PEG300	107 ± 12	23 ± 3	21 ± 4	42 ± 2

PHBHV/1%EG	62 ± 2	13 ± 1	21 ± 2	42 ± 2
PHBHV/2%PEG300	54 ± 13	No finger like structure		43 ± 2
PHBHV/2%EG	103 ± 5	No finger like structure		43 ± 2
PHBHV/5%PEG300	73 ± 7	No finger like structure		42 ± 2

No major trend is observed for the overall thicknesses of the membranes. And, in case of the membranes showing a finger like upper structure, the macrovoids account for the same thickness ratio, 21%. The interesting point is that despite the change of the dope solution composition and membrane morphology, the porosities show very similar values. Hence, the thickness variation cannot be explained by the porosity but rather by potential fluctuations during the casting process. However, if all the membranes show very similar porosity values, some changes on the pore size distribution can be observed on Figure 8.

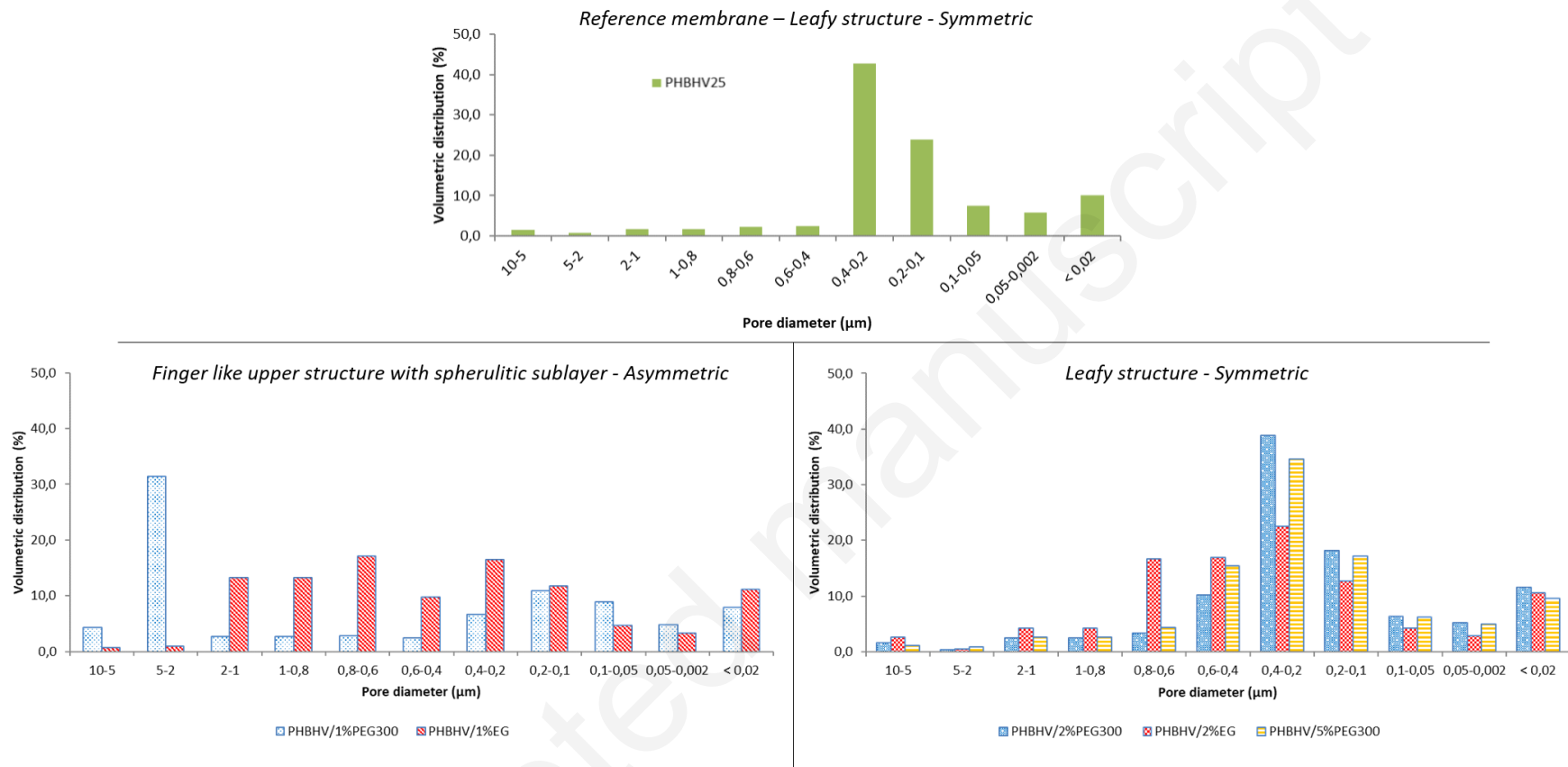


Figure 8: Pore size distribution of the different supported PHBHV based membranes.

The pore size distribution clearly distinguishes the symmetric membranes from the asymmetric membranes. In case of symmetric structures, the distributions display gaussian shapes with a main peak at 0.4-0.2 μm . While, for asymmetric structures, the distribution is spread over a wider range of pore size and the main difference is the presence of more pores above 0.8 μm . Thus, these bigger pores can be associated to the finger like macrovoids and interstitial spaces between spherulites.

Comparing the asymmetric structures, PHBHV/1%PEG300 membrane depicts the presence of bigger pores, around 5-2 μm , compared to PHBHV/1%EG membrane. That correlates with the bigger finger like macrovoids measured for the membrane with PEG300 (Table 6).

For the symmetric structures, the gaussian shape distribution is slightly extended to bigger pore sizes when additives are present while the reference membrane exhibits a very low volumetric distribution associated to the pores above 0.4 μm . The membranes with additives have a volumetric distribution superior to 10% for pore sizes up to 0.6 or 0.8 μm .

Hence, by using these additives from 1 to 5 wt%, the overall porosity never changed (Table 6) but the membrane morphology was affected and the consequences were either the formation of asymmetric structures or an increased pore size within the symmetric structures (Figure 8). The increasing of the porosity by adding such compounds is usually favored in case of higher additive/polymer ratios and higher additive molecular weights [76,78,85-87]. Hence, it could be argued that these concentrations and molecular weights are not enough to have a significant impact on the overall porosity. Yet, the membrane morphology was impacted and, as mentioned above, it can be explained by their effect on the solvent/non-solvent exchange rate.

At the end, these pore size ranges are usually what is expected for MF membranes [88]. The membranes performances were analyzed by water permeability and rejection of a kaolin dispersion. The results are displayed on Figure 9.

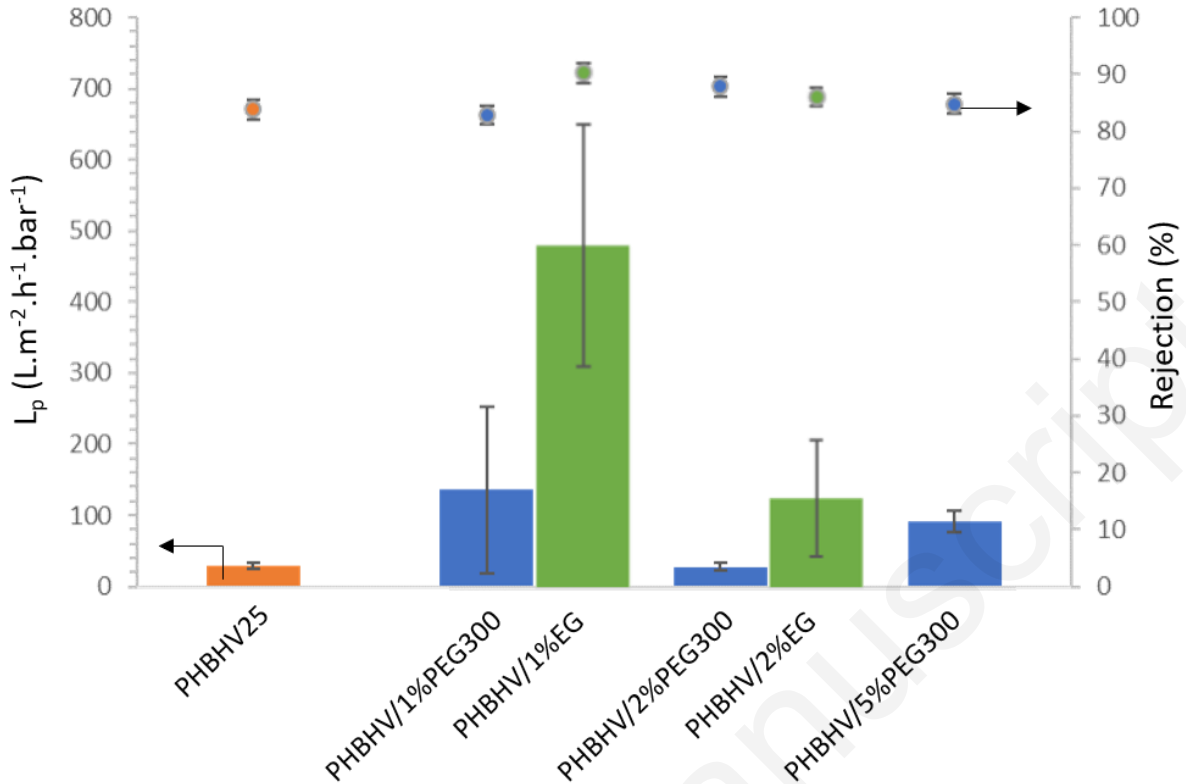


Figure 9: Filtration performances of the different supported PHBV based membranes.

The rejections are of the same order of magnitude for these membranes and is within the range of 80-90% for particles of kaolin having a mean size of $0.65 \mu m$. For MF membranes, the top surface pores are mainly responsible of the rejection efficiency and no major differences, from the surface images, could be depicted for these membranes. These decent rejection results emphasize the potential of such PHA based membranes.

By adding PEG300 and EG the permeability was greatly improved in most of the cases. The permeability seems to be quite dependent of the overall membrane structure. Indeed, the membranes with asymmetric structure, PHBV/1%PEG300 and PHBV/1%EG, show the best permeability results, respectively 135 and $480 L \cdot m^{-2} \cdot h^{-1} \cdot bar^{-1}$. It is in agreement with their bigger pore sizes (Figure 8). The potentially less tortuous pathway given by the finger like macrovoids would favor higher permeabilities. But they are also the ones with the biggest deviations. As mentioned previously, macrovoids and spherulitic layers are not suitable from a mechanical point a view [63,69], hence the permeability stability can be more impacted. For the symmetric membranes, PHBV/2%PEG300, PHBV/2%EG and PHBV/5%PEG, the best permeabilities are around $100 L \cdot m^{-2} \cdot h^{-1} \cdot bar^{-1}$. The membranes displaying this permeability, PHBV/2%EG and PHBV/5%PEG, are the one with more pores superior to $0.4 \mu m$.

4. Conclusion

This study was aimed to investigate the common phase inversion process to make a new biobased PHA membrane. The impact of the polymer concentration on the microstructure was studied and asymmetric structures with porous top layers were obtained. The macrovoids size was increased by increasing the PHBHV concentration. Within the prospect to improve the strength of the structure, membranes were then prepared on a non-woven support. The presence of the support greatly impacted the membrane morphology by promoting a S-L demixing and led to a symmetric leafy structure. In addition to the non-woven support, this type of symmetric structure is more suitable for better mechanical properties. Again, the influence of the PHBHV concentration was studied and the best reference membrane was set for a concentration of 25 wt%. The membranes microstructures were then strongly influenced by the addition of hydrophilic additives and asymmetric to symmetric structures were achieved. Asymmetric structures are promoted for low addition of PEG300 or EG, 1 wt%, while symmetric structures are then re-obtained for higher concentrations. The membranes show decent rejection values but, in this study, not influenced by the membrane microstructure. However, the permeabilities were greatly dependent of the membrane microstructure and the values were improved with the additives. This enhancement was related to an increased pore size.

At the end, this study gives a first insight of how to implement PHAs in a typical membrane fabrication process. It demonstrates that because of its particular properties, like its high crystallinity degree, it can behave differently to the common polymers during the phase inversion. However, after development of the process, biobased PHBHV membranes were successfully produced by NIPS. A such biobased and biodegradable material could be a good choice for the fabrication of disposable membrane systems.

5. Conflicts of interest

There are no conflicts to declare.

6. Acknowledgements

Francis Gouttefangeas and Loïc Joanny are acknowledged for SEM images performed at CMEBA (ScanMAT, University of Rennes 1) which received a financial support from the European Union (CPER-FEDER 2007-2014). Dr. Sylvain Giraudet is acknowledged for his assistance for pore size distribution determination. The Freudenberg company (Germany) is acknowledged for kindly providing the non-woven support.

7. References

- [1] S.P. Nunes, P.Z. Culfaz-Emecen, G.Z. Ramon, T. Visser, G.H. Koops, W. Jin, M. Ulbricht, Thinking the future of membranes: Perspectives for advanced and new membrane materials and manufacturing processes, *J. Memb. Sci.* 598 (2020). <https://doi.org/10.1016/j.memsci.2019.117761>.
- [2] S. Loeb, S. Sourirajan, Sea Water Demineralization by Means of an Osmotic Membrane, in: 1963: pp. 117-132. <https://doi.org/10.1021/ba-1963-0038.ch009>.
- [3] J. Hennessy, A. Livingston, R. Baker, Membranes from academia to industry, *Nat. Mater.* 16 (2017) 280-282. <https://doi.org/10.1038/nmat4861>.
- [4] The future of plastic, *Nat. Commun.* 9 (2018). <https://doi.org/10.1038/s41467-018-04565-2>.
- [5] J. Gigault, B. Pedrono, B. Maxit, A. ter halle, Marine plastic litter: The unanalyzed nano-fraction, *Environ. Sci. Nano.* 3 (2016).
- [6] Y. Zhu, C. Romain, C.K. Williams, Sustainable polymers from renewable resources, *Nature.* 540 (2016) 354-362. <https://doi.org/10.1038/nature21001>.
- [7] S. Jiang, B.P. Ladewig, Green synthesis of polymeric membranes: recent advances and future prospects, *Curr. Opin. Green Sustain. Chem.* (2019). <https://doi.org/10.1016/J.COCS.2019.07.002>.
- [8] A.G. Livingston, G. Szekely, M.F. Jimenez-Solomon, P. Marchetti, J.F. Kim, Sustainability assessment of organic solvent nanofiltration: from fabrication to application, *Green Chem.* 16 (2014) 4440. <https://doi.org/10.1039/c4gc00701h>.
- [9] F. Galiano, K. Briceño, T. Marino, A. Molino, K.V. Christensen, A. Figoli, Advances in biopolymer-based membrane preparation and applications, *J. Memb. Sci.* 564 (2018) 562-586. <https://doi.org/10.1016/J.MEMSCI.2018.07.059>.
- [10] T. Tanaka, D.R. Lloyd, Formation of poly(l-lactic acid) microfiltration membranes via thermally induced phase separation, *J. Memb. Sci.* 238 (2004) 65-73. <https://doi.org/10.1016/J.MEMSCI.2004.03.020>.
- [11] A.C. Chinyerenwa, H. Wang, Q. Zhang, Y. Zhuang, K.H. Munna, C. Ying, H. Yang, W. Xu, Structure and thermal properties of porous polylactic acid membranes prepared via phase inversion induced by hot water droplets, *Polymer (Guildf)*. 141 (2018) 62-69. <https://doi.org/10.1016/J.POLYMER.2018.03.011>.
- [12] Z. Xiong, H. Lin, F. Liu, X. Yu, Y. Wang, Y. Wang, A new strategy to simultaneously improve the permeability, heat-deformation resistance and antifouling properties of polylactide membrane via bio-based β -cyclodextrin and surface

- crosslinking, *J. Memb. Sci.* 513 (2016) 166–176.
<https://doi.org/10.1016/j.memsci.2016.04.036>.
- [13] Q. Xing, X. Dong, R. Li, H. Yang, C.C. Han, D. Wang, Morphology and performance control of PLLA-based porous membranes by phase separation, *Polymer (Guildf)*. 54 (2013) 5965–5973.
<https://doi.org/10.1016/j.polymer.2013.08.007>.
- [14] V. Ghaffarian, S.M. Mousavi, M. Bahreini, H. Jalaei, Polyethersulfone/poly (butylene succinate) membrane: Effect of preparation conditions on properties and performance, *J. Ind. Eng. Chem.* 20 (2014) 1359–1366.
<https://doi.org/10.1016/j.jiec.2013.07.019>.
- [15] Keita Kashima and Masanao Imai, Advanced Membrane Material from Marine Biological Polymer and Sensitive Molecular-Size Recognition for Promising Separation Technology, in: *Adv. Desalin.*, 2012: p. 224.
<https://doi.org/dx.doi.org/10.5772/50734>.
- [16] F. Liu, B. Qin, L. He, R. Song, Novel starch/chitosan blending membrane: Antibacterial, permeable and mechanical properties, *Carbohydr. Polym.* 78 (2009) 146–150.
<https://doi.org/10.1016/J.CARBPOL.2009.03.021>.
- [17] F. Suzuki, H. Kimura, T. Shibue, Formation having a tanning gradient structure of collagen membrane by the pervaporation technique, *J. Memb. Sci.* 165 (2000) 169–175.
[https://doi.org/10.1016/S0376-7388\(99\)00233-1](https://doi.org/10.1016/S0376-7388(99)00233-1).
- [18] P. Wu, M. Imai, Novel Biopolymer Composite Membrane Involved with Selective Mass Transfer and Excellent Water Permeability, in: *Adv. Desalin.*, 2012: p. 224. <https://doi.org/10.5772/50697>.
- [19] J.P. Chaudhary, S.K. Nataraj, A. Gogda, R. Meena, Bio-based superhydrophilic foam membranes for sustainable oil-water separation, *Green Chem.* (2014) 4552–4558.
<https://doi.org/10.1039/c4gc01070a>.
- [20] T.C. Mokhena, A.S. Luyt, Development of multifunctional nano/ultrafiltration membrane based on a chitosan thin film on alginate electrospun nanofibres, *J. Clean. Prod.* 156 (2017) 470–479. <https://doi.org/10.1016/j.jclepro.2017.04.073>.
- [21] V.K. Thakur, S.I. Voicu, Recent advances in cellulose and chitosan based membranes for water purification: A concise review, *Carbohydr. Polym.* 146 (2016) 148–165.
<https://doi.org/10.1016/j.carbpol.2016.03.030>.
- [22] F. Liu, B. Qin, L. He, R. Song, Novel starch/chitosan blending membrane: Antibacterial, permeable and mechanical properties, *Carbohydr. Polym.* 78 (2009) 146–150.
<https://doi.org/10.1016/J.CARBPOL.2009.03.021>.
- [23] S. Modi, K. Koelling, Y. Vodovotz, Assessment of PHB with varying hydroxyvalerate content for potential packaging applications, *Eur. Polym. J.* 47 (2011) 179–186.
<https://doi.org/10.1016/j.eurpolymj.2010.11.010>.

- [24] Y.M. Corre, S. Bruzaud, J.L. Audic, Y. Grohens, Morphology and functional properties of commercial polyhydroxyalkanoates: A comprehensive and comparative study, *Polym. Test.* 31 (2012) 226–235. <https://doi.org/10.1016/j.polymertesting.2011.11.002>.
- [25] L. Shen, J. Haufe, M.K. Patel, Product overview and market projection of emerging bio-based plastics, 2009. www.chem.uu.nl/nswwww.copernicus.uu.nl/commissionedbyEuropeanPolysaccharideNetworkofExcellence (accessed May 20, 2019).
- [26] G.-Q. Chen, A microbial polyhydroxyalkanoates (PHA) based bio- and materials industry, *Chem. Soc. Rev.* 38 (2009) 2434. <https://doi.org/10.1039/b812677c>.
- [27] Tepha Inc., Medical devices and applications of polyhydroxyalkanoate polymers, US7553923B2, 2009. <https://patentimages.storage.googleapis.com/1c/9e/0c/1cfbe75517ca50/US7553923.pdf> (accessed July 19, 2019).
- [28] A. Shrivastav, H.-Y. Kim, Y.-R. Kim, Advances in the applications of polyhydroxyalkanoate nanoparticles for novel drug delivery system., *Biomed Res. Int.* (2013). <https://doi.org/10.1155/2013/581684>.
- [29] G.-Q. Chen, Q. Wu, The application of polyhydroxyalkanoates as tissue engineering materials, *Biomaterials.* 26 (2005) 6565–6578. <https://doi.org/10.1016/J.BIOMATERIALS.2005.04.036>.
- [30] P.E. Grimes, B.A. Green, R.H. Wildnauer, B.L. Edison, The use of polyhydroxy acids (PHAs) in photoaged skin., *Cutis.* 73 (2004) 3–13. <http://www.ncbi.nlm.nih.gov/pubmed/15002656> (accessed July 23, 2019).
- [31] L. Hartley Yee, L.J. Ray Foster, Polyhydroxyalkanoates as Packaging Materials: Current Applications and Future Prospects, in: *Polyhydroxyalkanoate Based Blends, Compos. Nanocomposites*, Royal Society of Chemistry, 2014: pp. 183–207. <https://doi.org/10.1039/9781782622314-00183>.
- [32] A.M. Díez-Pascual, A.L. Díez-Vicente, ZnO-Reinforced Poly(3-hydroxybutyrate-co-3-hydroxyvalerate) Bionanocomposites with Antimicrobial Function for Food Packaging, *ACS Appl. Mater. Interfaces.* 6 (2014) 9822–9834. <https://doi.org/10.1021/am502261e>.
- [33] E. Bugnicourt, P. Cinelli, A. Lazzeri, V. Alvarez, Polyhydroxyalkanoate (PHA): Review of synthesis, characteristics, processing and potential applications in packaging, *Express Polym. Lett.* 8 (2014) 791–808. <https://doi.org/10.3144/expresspolymlett.2014.82>.
- [34] P. Ragaert, M. Buntinx, C. Maes, C. Vanheusden, R. Peeters, S. Wang, D.R. D'hooge, L. Cardon, Polyhydroxyalkanoates for Food Packaging Applications, in: *Ref. Modul. Food Sci.*, Elsevier, 2019. <https://doi.org/10.1016/B978-0-08-100596-5.22502-X>.
- [35] Buggi Toys GmbH, toy building block, DE102010004338A1, 2010. <https://patents.google.com/patent/DE102010004338A1/en> (accessed

July 19, 2019).

- [36] A. Marcano, O. Ba, P. Thebault, R. Crétois, Elucidation of innovative antibiofilm materials, *Colloids Surfaces B Biointerfaces*. 136 (2015) 56-63.
- [37] A. Marcano, N. Bou Haidar, S. Marais, J.-M. Valleton, A.C. Duncan, Designing Biodegradable PHA-Based 3D Scaffolds with Antibiofilm Properties for Wound Dressings: Optimization of the Microstructure/Nanostructure, *ACS Biomater. Sci. Eng.* 3 (2017) 3654-3661. <https://doi.org/10.1021/acsbiomaterials.7b00552>.
- [38] J. Xi, J. Li, L. Zhu, Y. Gong, N. Zhao, X. Zhang, Effects of Quenching Temperature and Time on Pore Diameter of Poly (3-hydroxybutyrate- co -3-hydroxyhexanoate) Porous Scaffolds and MC3T3-E1 Osteoblast Response to the Scaffolds, *Tsinghua Sci. Technol.* 12 (2007) 366-371.
- [39] D. Guzman, H. Kirsebom, C. Solano, J. Quillaguama, R. Hattikaul, Preparation of hydrophilic poly(3-hydroxybutyrate) macroporous scaffolds through enzyme-mediated modifications, *J. Bioact. Compat. Polym.* 26 (2011) 452-463. <https://doi.org/10.1177/0883911511419970>.
- [40] A. Mas, H. Jaaba, J. Sledz, F. Schue, Membranes en PHB, P(HB-co-9% HV), P(HB-co-22% HV) pour la microfiltration ou la pervaporation propriétés filtrantes et état de surface, *Eur. Polym. J.* 32 (1996) 435-450.
- [41] M. Villegas, E.F. Castro, A.C. Habert, J.C. Gottifredi, Sorption and pervaporation with poly (3-hydroxybutyrate) membranes : methanol / methyl tertbutyl ether mixtures, *J. Memb. Sci.* 367 (2011) 103-109. <https://doi.org/10.1016/j.memsci.2010.10.051>.
- [42] W.L. Tan, N.N. Yaakob, A. Zainal Abidin, M. Abu Bakar, N.H.H. Abu Bakar, Metal Chloride Induced Formation of Porous Polyhydroxybutyrate (PHB) Films : Morphology , Thermal Properties and Crystallinity, *IOP Conf. Ser. Mater. Sci. Eng.* 133 (2016). <https://doi.org/10.1088/1757-899X/133/1/012012>.
- [43] N. Follain, C. Chappay, E. Dargent, F. Chivrac, R. Crétois, S. Marais, Structure and Barrier Properties of Biodegradable Polyhydroxyalkanoate Films, *J. Phys. Chem.* 118 (2014) 6165-6177.
- [44] P. Taylor, A.L. Lordanskii, P.P. Kamaev, G.E. Zaikov, Water Sorption and Diffusion in Poly (3-hydroxybutyrate) Films, *Int. J. Polym. Mater. Polym. Biomater.* 41 (1998) 55-63. <https://doi.org/10.1080/00914039808034854>.
- [45] G. Torun Kose, H. Kenar, N. Hasırcı, V. Hasırcı, Macroporous poly (3-hydroxybutyrate- co -3-hydroxyvalerate) matrices for bone tissue engineering, *Biomaterials*. 24 (2003) 1949-1958. [https://doi.org/10.1016/S0142-9612\(02\)00613-0](https://doi.org/10.1016/S0142-9612(02)00613-0).
- [46] N. Wang, Z. Zhou, L. Xia, Y. Dai, H. Liu, Fabrication and characterization of bioactive β -Ca₂SiO₄/PHBV composite

- scaffolds, *Mater. Sci. Eng. C.* 33 (2013) 2294–2301.
<https://doi.org/10.1016/j.msec.2013.01.059>.
- [47] Y. Wang, Q. Wu, J. Chen, G. Chen, Evaluation of three-dimensional scaffolds made of blends of hydroxyapatite and poly(3-hydroxybutyrate-co-3-hydroxyhexanoate) for bone reconstruction, *Biomaterials.* 26 (2005) 899–904.
<https://doi.org/10.1016/j.biomaterials.2004.03.035>.
- [48] S.K. Misra, D. Mohn, T.J. Brunner, W.J. Stark, S.E. Philip, I. Roy, V. Salih, J.C. Knowles, A.R. Boccaccini, Comparison of nanoscale and microscale bioactive glass on the properties of P(3HB)/Bioglass composites, *Biomaterials.* 29 (2008) 1750–1761.
<https://doi.org/10.1016/j.biomaterials.2007.12.040>.
- [49] M. Dias, E.M.C. Moraes, A.R. Santos, J.E.M. Isabel, Blends of poly(3-hydroxybutyrate) and poly(p-dioxanone): miscibility, thermal stability and biocompatibility, *J. Mater. Sci. Mater. Med.* 19 (2008) 3535–3544. <https://doi.org/10.1007/s10856-008-3531-1>.
- [50] G. Cheng, Z. Cai, L. Wang, Biocompatibility and biodegradation of poly(hydroxybutyrate)/poly(ethylene glycol) blend films, *J. Mater. Sci. Mater. Med.* 14 (2003) 1073–1078.
- [51] J. Kang, H. Gi, R. Choe, S. Il Yun, Fabrication and characterization of poly(3-hydroxybutyrate) gels using non-solvent-induced phase separation, *Polymer (Guildf).* 104 (2016) 61–71. <https://doi.org/10.1016/j.polymer.2016.09.093>.
- [52] R.T.H. Chan, H. Marc, T. Ahmed, R.A. Russell, J. Holden, L.J.R. Foster, Poly(ethylene glycol) -modulated cellular biocompatibility of polyhydroxyalkanoate films, *Polym. Int.* 62 (2013) 884–892. <https://doi.org/10.1002/pi.4451>.
- [53] H.S. Barud, J.L. Souza, D.B. Santos, M.S. Crespi, C.A. Ribeiro, Y. Messaddeq, S.J.L. Ribeiro, Bacterial cellulose/poly(3-hydroxybutyrate) composite membranes, *Carbohydr. Polym.* 83 (2011) 1279–1284.
<https://doi.org/10.1016/j.carbpol.2010.09.049>.
- [54] A.A. Kehail, C.J. Brigham, Anti-biofilm Activity of Solvent-Cast and Electrospun Polyhydroxyalkanoate Membranes Treated with Lysozyme, *J. Polym. Environ.* 26 (2017) 66–72.
<https://doi.org/10.1007/s10924-016-0921-1>.
- [55] A.R.S. Jr, B.M.P. Ferreira, E.A.R. Duek, H. Dolder, R.S. Wada, M.L.F. Wada, Differentiation Pattern of Vero Cells Cultured on Poly(L-Lactic Acid)/Poly(Hydroxybutyrate-co-Hydroxyvalerate) Blends, *Artif. Organs.* 28 (2004) 381–389.
- [56] N. Jacquél, C.-W. Lo, H.-S. Wu, Y.-H. Wei, S.S. Wang, Solubility of Polyhydroxyalkanoates by Experiment and Thermodynamic Correlations, *AIChE J.* 53 (2007) 2704–2714.
<https://doi.org/10.1002/aic>.
- [57] H.H. Wang, J.T. Jung, J.F. Kim, S. Kim, E. Drioli, Y.M. Lee, A novel green solvent alternative for polymeric membrane

- preparation via nonsolvent-induced phase separation (NIPS), *J. Memb. Sci.* 574 (2019) 44-54.
<https://doi.org/10.1016/j.memsci.2018.12.051>.
- [58] C. Özdemir, A. Güner, Solubility profiles of poly(ethylene glycol)/solvent systems, I: Qualitative comparison of solubility parameter approaches, *Eur. Polym. J.* 43 (2007) 3068-3093. <https://doi.org/10.1016/j.eurpolymj.2007.02.022>.
- [59] D.W. van (Dirk W. Krevelen, K. te. Nijenhuis, *Properties of polymers : their correlation with chemical structure ; their numerical estimation and prediction from additive group contributions*, Elsevier, 2009.
- [60] M. Terada, R.H. Marchessault, Determination of solubility parameters for poly (3-hydroxyalkanoates), *Int. J. Biol. Macromol.* 25 (1999) 207-215.
- [61] B. Liu, Q. Du, Y. Yang, The phase diagrams of mixtures of EVAL and PEG in relation to membrane formation, *J. Memb. Sci.* 180 (2000) 81-92. [https://doi.org/10.1016/S0376-7388\(00\)00526-3](https://doi.org/10.1016/S0376-7388(00)00526-3).
- [62] G.R. Guillen, Y. Pan, M. Li, E.M. V. Hoek, Preparation and Characterization of Membranes Formed by Nonsolvent Induced Phase Separation: A Review, *Ind. Eng. Chem. Res.* 50 (2011) 3798-3817. <https://doi.org/10.1021/ie101928r>.
- [63] J. Tae, J.F. Kim, H. Hyun, E. Drioli, Y. Moo, Understanding the non-solvent induced phase separation (NIPS) effect during the fabrication of microporous PVDF membranes via thermally induced phase separation (TIPS), *J. Memb. Sci.* 514 (2016) 250-263.
<https://doi.org/10.1016/j.memsci.2016.04.069>.
- [64] C.A. Smolders, A.J. Reuvers, R.M. Boom, I.M. Wienk, Microstructures in phase-inversion membranes. Part 1. Formation of macrovoids, *J. Memb. Sci.* 73 (1992) 259-275.
[https://doi.org/10.1016/0376-7388\(92\)80134-6](https://doi.org/10.1016/0376-7388(92)80134-6).
- [65] B.S. Lalia, V. Kochkodan, R. Hashaikeh, N. Hilal, A review on membrane fabrication: Structure, properties and performance relationship, *Desalination.* 326 (2013) 77-95.
<https://doi.org/10.1016/j.desal.2013.06.016>.
- [66] P. Van De Witte, P.J. Dijkstra, J.W.A. Van Den Berg, J. Feijen, Phase separation processes in polymer solutions in relation to membrane formation, *J. Memb. Sci.* 117 (1996) 1-31.
[https://doi.org/10.1016/0376-7388\(96\)00088-9](https://doi.org/10.1016/0376-7388(96)00088-9).
- [67] H. Strathmann, K. Kock, P. Amar, R.W. Baker, The formation mechanism of asymmetric membranes, *Desalination.* 16 (1975) 179-203. [https://doi.org/10.1016/S0011-9164\(00\)82092-5](https://doi.org/10.1016/S0011-9164(00)82092-5).
- [68] L. Broens, P.W. Altena, C.A. Smolders, Asymmetric membrane structures as a result of phase separation phenomena, *Desalination.* 32 (1980) 33-45.
- [69] Hui-An Tsai, Doan-Ho Huang, R.-C. Ruaan, J.-Y. Lai, Mechanical Properties of Asymmetric Polysulfone Membranes Containing

- Surfactant as Additives, *Ind. Eng. Chem. Res.* 40 (2001) 5917-5922. <https://doi.org/10.1021/IE010026E>.
- [70] D.R. Lloyd, K.E. Kinzer, H.S. Tseng, Microporous membrane formation via thermally induced phase separation. I. Solid-liquid phase separation, *J. Memb. Sci.* 52 (1990) 239-261. [https://doi.org/10.1016/S0376-7388\(00\)85130-3](https://doi.org/10.1016/S0376-7388(00)85130-3).
- [71] T.H. Young, L.P. Cheng, D.J. Lin, L. Fane, W.Y. Chuang, Mechanisms of PVDF membrane formation by immersion-precipitation in soft (1-octanol) and harsh (water) nonsolvents, *Polymer (Guildf)*. 40 (1999) 5315-5323. [https://doi.org/10.1016/S0032-3861\(98\)00747-2](https://doi.org/10.1016/S0032-3861(98)00747-2).
- [72] J. Yang, D.W. Li, Y.K. Lin, X.L. Wang, F. Tian, Z. Wang, Formation of a bicontinuous structure membrane of polyvinylidene fluoride in diphenyl ketone diluent via thermally induced phase separation, *J. Appl. Polym. Sci.* 110 (2008) 341-347. <https://doi.org/10.1002/app.28606>.
- [73] S. ichi Sawada, C. Ursino, F. Galiano, S. Simone, E. Drioli, A. Figoli, Effect of citrate-based non-toxic solvents on poly(vinylidene fluoride) membrane preparation via thermally induced phase separation, *J. Memb. Sci.* 493 (2015) 232-242. <https://doi.org/10.1016/j.memsci.2015.07.003>.
- [74] C.W.J. Mcchalicher, F. Srienc, D.P. Rouse, Solubility and Degradation of Polyhydroxyalkanoate Biopolymers in Propylene Carbonate, *AIChE J.* 56 (2009) 1616-1625. <https://doi.org/10.1002/aic.12087>.
- [75] W. Ma, J. Zhang, B. Van der Bruggen, X. Wang, Formation of an interconnected lamellar structure in PVDF membranes with nanoparticles addition via solid-liquid thermally induced phase separation, *J. Appl. Polym. Sci.* 127 (2013) 2715-2723. <https://doi.org/10.1002/app.37574>.
- [76] Y. Ma, F. Shi, J. Ma, M. Wu, J. Zhang, C. Gao, Effect of PEG additive on the morphology and performance of polysulfone ultrafiltration membranes, *Desalination*. 272 (2011) 51-58. <https://doi.org/10.1016/J.DESAL.2010.12.054>.
- [77] M. Amirilargani, T. Mohammadi, Effects of PEG on morphology and permeation properties of polyethersulfone membranes, *Sep. Sci. Technol.* 44 (2009) 3854-3875. <https://doi.org/10.1080/01496390903182347>.
- [78] B. Chakrabarty, A.K. Ghoshal, M.K. Purkait, Effect of molecular weight of PEG on membrane morphology and transport properties, *J. Memb. Sci.* 309 (2008) 209-221. <https://doi.org/10.1016/j.memsci.2007.10.027>.
- [79] S. Rekha Panda, S. De, Role of polyethylene glycol with different solvents for tailor-made polysulfone membranes, *J. Polym. Res.* 20 (2013). <https://doi.org/10.1007/s10965-013-0179-4>.
- [80] Z.L. Xu, T.S. Chung, K.C. Loh, B.C. Lim, Polymeric asymmetric

- membranes made from polyetherimide/polybenzimidazole/poly(ethylene glycol) (PEI/PBI/PEG) for oil-surfactant-water separation, *J. Memb. Sci.* 158 (1999) 41-53. [https://doi.org/10.1016/S0376-7388\(99\)00030-7](https://doi.org/10.1016/S0376-7388(99)00030-7).
- [81] D.F. Parra, J. Fusaro, F. Gaboardi, D.S. Rosa, Influence of poly (ethylene glycol) on the thermal, mechanical, morphological, physical-chemical and biodegradation properties of poly (3-hydroxybutyrate), *Polym. Degrad. Stab.* 91 (2006) 1954-1959. <https://doi.org/10.1016/j.polyimdegradstab.2006.02.008>.
- [82] R. Requena, A. Jiménez, M. Vargas, A. Chiralt, Effect of plasticizers on thermal and physical properties of compression-moulded poly[(3-hydroxybutyrate)-co-(3-hydroxyvalerate)] films, *Polym. Test.* 56 (2016) 45-53. <https://doi.org/10.1016/J.POLYMERTESTING.2016.09.022>.
- [83] F. Liu, N.A. Hashim, Y. Liu, M.R.M. Abed, K. Li, Progress in the production and modification of PVDF membranes, *J. Memb. Sci.* 375 (2011) 1-27. <https://doi.org/10.1016/j.memsci.2011.03.014>.
- [84] W.L. Chou, D.G. Yu, M.C. Yang, C.H. Jou, Effect of molecular weight and concentration of PEG additives on morphology and permeation performance of cellulose acetate hollow fibers, *Sep. Purif. Technol.* 57 (2007) 209-219. <https://doi.org/10.1016/j.seppur.2007.04.005>.
- [85] E. Saljoughi, T. Mohammadi, Cellulose acetate (CA)/polyvinylpyrrolidone (PVP) blend asymmetric membranes: Preparation, morphology and performance, *Desalination.* 249 (2009) 850-854. <https://doi.org/10.1016/j.desal.2008.12.066>.
- [86] B. Chakrabarty, A.K. Ghoshal, M.K. Purkait, Preparation, characterization and performance studies of polysulfone membranes using PVP as an additive, *J. Memb. Sci.* 315 (2008) 36-47. <https://doi.org/10.1016/j.memsci.2008.02.027>.
- [87] A. Idris, N. Mat Zain, M.Y. Noordin, Synthesis, characterization and performance of asymmetric polyethersulfone (PES) ultrafiltration membranes with polyethylene glycol of different molecular weights as additives, *Desalination.* 207 (2007) 324-339. <https://doi.org/10.1016/j.desal.2006.08.008>.
- [88] R. Sahai, MEMBRANE SEPARATIONS | Filtration, in: *Encycl. Sep. Sci.*, Elsevier, 2000: pp. 1717-1724. <https://doi.org/10.1016/b0-12-226770-2/05151-6>.

Declaration of interests

The authors declare that they have no known competing financial interests or personal relationships that could have appeared to influence the work reported in this paper.

The authors declare the following financial interests/personal relationships which may be considered as potential competing interests:

Accepted manuscript